Chapter 4: Effective treatment of steatosis and steatohepatitis by fibroblast growth factor 1 in mouse models of non-alcoholic fatty liver disease

Weilin Liu[a], **Dicky Struik[a]**, Vera J.M. Nies[a], Angelika Jurdzinski[a], Liesbeth Harkema[b], Alain de Bruin[a,b], Henkjan J. Verkade[a], Michael Downes[c], Ronald M. Evans[c], Tim van Zutphen[a], and Johan W. Jonker[a]

[a]Center for Liver, Digestive and Metabolic Diseases, Department of Pediatrics, University of Groningen, University Medical Center Groningen, Hanzeplein 1, 9713 GZ Groningen, The Netherlands.
[b]Dutch Molecular Pathology Center, Faculty of Veterinary Medicine, Utrecht University, Yalelaan 1, 3584 CL Utrecht, The Netherlands.
[c]Gene Expression Laboratory, Salk Institute for Biological Studies, 10010 North Torrey Pines Road, La Jolla, California 92037, USA.

Proc Natl Acad Sci USA, 2016, 113(8):228-93.

Abstract

Non-alcoholic fatty liver disease (NAFLD) is the most common chronic liver disorder and strongly associated with obesity and type 2 diabetes. Currently, there is no approved pharmacological treatment for this disease but improvement of insulin resistance using PPARγ agonists, such as thiazolidinediones (TZDs), has been shown to effectively reduce steatosis, steatohepatitis and improve liver function in patients with obesity-related NAFLD. However, this approach is limited by adverse effects of TZDs.

Recently, we have identified fibroblast growth factor 1 (FGF1) as a target of nuclear receptor PPARγ in visceral adipose tissue and as a critical factor in adipose remodeling. As FGF1 is situated downstream of PPARγ, it is likely that therapeutic targeting of the FGF1 pathway will eliminate some of the serious adverse effects associated with TZDs.

Here we show that pharmacological administration of recombinant FGF1 (rFGF1) effectively improves hepatic inflammation and damage in leptin-deficient *ob/ob* mice and in choline-deficient mice, two etiologically different models of NAFLD. Hepatic steatosis was only effectively reduced in *ob/ob* mice, suggesting that rFGF1 stimulates hepatic lipid catabolism. Potentially adverse effects such as fibrosis or proliferation were not observed in these models. Since the anti-inflammatory effects were observed both in the presence and absence of the anti-steatotic effects, our findings further suggest that the anti-inflammatory property of rFGF1 is independent from its effect on lipid catabolism. In addition to its potent glucose-lowering and insulin-sensitizing effects, our current findings indicate that rFGF1 could also be therapeutically effective in the treatment of NAFLD.

Significance

Fibroblast growth factor 1 (FGF1) is critical for adipose tissue remodeling under conditions of dietary stress. Pharmacological treatment with recombinant FGF1 (rFGF1) has potent glucose-lowering, insulin-sensitizing and anti-steatotic effects in hyperglycemic mouse models, yet the mechanism is largely unknown. Here, we characterized the effects of rFGF1 on non-alcoholic liver disease in two etiologically different mouse models. Whereas strong anti-steatotic effects of rFGF1 were observed in *ob/ob* mice, this was not observed in choline-deficient mice, suggesting that rFGF1 exerts its anti-steatotic effect via processes specifically impaired in choline-deficient mice, such as lipid oxidation and lipoprotein secretion. In contrast, hepatic inflammation and alanine aminotransferase levels were reduced in both models, indicating that these effects are independent of the anti-steatotic properties of rFGF1.

Introduction

Non-alcoholic fatty liver disease (NAFLD) is the most common chronic liver disease in developed countries and strongly associated with obesity and type 2 diabetes (1). NAFLD refers to a wide spectrum of liver disorders ranging from simple fatty liver (steatosis) to nonalcoholic steatohepatitis (NASH) with increased risk to develop progressive fibrosis, cirrhosis and liver cancer (2).

Treatment options for NAFLD are limited and mainly directed at weight loss or pharmacological improvement of insulin resistance (3). While no pharmacologic therapy has been approved, the thiazolidinedione (TZD) class of insulin sensitizers has been demonstrated to improve steatosis, steatohepatitis and liver function in mice and patients with NAFLD (1). TZDs improve insulin sensitivity through activation of nuclear receptor peroxisome proliferator-activated receptor-gamma (PPARy) which reduces insulin resistance in adipose tissue, liver and skeletal muscle (4). The exact mechanism by which PPARy exerts its beneficial effects on NAFLD is not completely understood but it is believed that improved hepatic insulin sensitivity enhances lipid oxidation and reduces hepatic lipogenesis, thereby reducing steatosis (5). In addition, increased peripheral insulin sensitivity may reduce lipolysis in white adipose tissue and thereby limit ectopic fat accretion.

PPARy and its activators also have broad anti-inflammatory effects. On one hand PPARy has been shown to attenuate the expression and secretion of pro-inflammatory cytokines (including IL-1β and TNF-α) associated with M1 macrophages (6) whereas on the other hand it reduces macrophage activity via transrepression of nuclear factor-κB (7). Despite their efficacy in glycemic control and reduction of steatosis, TZDs are associated with various serious adverse side effects, including weight gain, fluid retention, osteoporosis and cardiovascular toxicity, which has strongly limited their clinical use (4). These limitations highlight the need for novel approaches such as more selective PPARy agonists or through direct activation of downstream targets.

Recently, we have identified fibroblast growth factor 1 (FGF1) as a novel target of PPARγ in visceral adipose tissue and as a critical factor in adipose remodeling (8). Mice with a deficiency in FGF1 displayed a severe diabetic phenotype with increased inflammation and fibrosis in adipose tissue. Conversely, pharmacological treatment with rFGF1 has a potent insulin-sensitizing effect at the systemic level, whereas in the liver it effectively reduces steatosis in *ob/ob* mice (9). It remains unclear, however, if and to what extent the hepatic effects of FGF1 are direct or indirect.

In this study, we aimed to determine the mechanism by which rFGF1 improves liver disease using two etiologically different models of NAFLD. First, leptin-deficient *ob/ob* mice, which develop steatosis primarily through excessive food intake, and second, mice with a dietary choline-deficiency, which develop steatosis primarily as a result of a defect in hepatic lipid catabolism (10). Interestingly, we found that rFGF1 effectively reverses steatosis in *ob/ob* mice but not in mice with a dietary choline-deficiency, suggesting that rFGF1 stimulates hepatic lipid catabolism. rFGF1 treatment improved steatohepatitis and plasma alanine transaminase activity (ALT) in both models, indicating that effects of rFGF1 on hepatic inflammation and liver function are independent from its anti-steatotic properties. Together our results provide insight into the mechanism by which rFGF1 improves NAFLD and highlight its potential therapeutic value in the treatment of different aspects of liver disease.

Results

rFGF1 has potent anti-steatotic effects in *ob/ob* mice. To investigate the mechanism by which rFGF1 exerts its effects on NAFLD/NASH we treated *ob/ob* mice for a period of 12 days with rFGF1 (0.5 mg/kg i.p. every 3 days). Twelve days of treatment significantly reduced hepatic levels of triglycerides and liver mass, without affecting body weight (**Fig. 1*A-C***). Histological examination using haematoxylin and eosin (H&E) staining confirmed the anti-steatotic effect of rFGF1 but also revealed that this reduction in hepatic lipids occurred in a zonated fashion (**Fig. 1*D***). To further explore this zonation effect, we used the central vein (CV) marker glutamine synthetase (GS), which indicated pronounced reduction of steatosis in the periportal (PP) zone, while steatosis in the pericentral (PC) region was not significantly affected by rFGF1 treatment (**Fig. 1*E-G***).

rFGF1 suppresses hepatic inflammation in *ob/ob* mice. Hepatic steatosis can develop into non-alcoholic steatohepatitis (NASH), which is more serious and is characterized by hepatic inflammation and fibrosis. In addition to its potent anti-steatotic action, rFGF1 also suppressed hepatic inflammation in *ob/ob* mice as indicated by reduced mRNA expression of a range of hepatic inflammatory markers (**Fig. 2*A-D***). Twelve days of treatment with rFGF1 significantly reduced the expression of the pro-inflammatory M1 markers *MCP-1* and *TNFα*, and macrophage/Kupffer markers *F4/80*, *CD68* and *CD11c* (**Fig. 2*A***). After 5 wks of treatment with rFGF1 these markers were even further reduced and significant reductions were now also observed for the pro-inflammatory cytokine *IL1β*, cell adhesion molecules *E-selectin*, *ICAM-1* and *VCAM-1*, which are activated by TNFα and IL-1β, and the macrophage marker *CD11b* (**Fig. 2*B***). In contrast, hepatic expression of anti-inflammatory M2 markers *IL-10*, *CD163* and Arginase 1 (*Arg1*) was not affected by rFGF1 administration, except for *CD206* in the 5 wk treated mice (**Fig. S1*A-D***), indicating that rFGF1 exerts its anti-inflammatory effect mainly through suppression of pro-inflammatory M1 markers in liver. Reduced hepatic inflammation was also observed by histopathological and protein analysis, indicating lower scores on lobular inflammation (**Table S1**) and reduced levels of TNFα (**Fig. 2*C-E***).

rFGF1 reduces endothelial *VCAM-1* expression. To investigate how rFGF1 suppresses hepatic inflammation we examined its potential to modulate cytokine- or endotoxin-induced inflammatory gene expression in several cell models representing different hepatic cell types (hepatocytes, macrophages and endothelial cells). We did not find a role for hepatocytes, the major parenchymal cell type in liver, in the anti-inflammatory effect of rFGF1 as it did not affect basal and even slightly increased cytokine-induced (*i.e.* TNFα/IL1β) inflammatory gene expression (**Fig. S2**). We next questioned if rFGF1 could mediate its anti-inflammatory effect through modulation of endotoxin-induced activation of macrophages or endothelial cells. We examined the effect of rFGF1 pre-incubation on the activation of RAW264.7 macrophage cells and HUVEC endothelial cells by lipopolysaccharide (LPS). In RAW264.7 cells, rFGF1 pre-treatment did not interfere with basal or endotoxin-induced inflammatory gene expression (**Fig. S2**). In contrast, a significant reduction in the expression of VCAM-1 was observed in HUVECs in response to LPS (**Fig. 3*A***). Basal and endotoxin-induced gene expression of *MCP-1*, *ICAM-1* and *E-selectin* was unaffected by rFGF1 pre-treatment in HUVECs (**Fig. 3*B-D***). Since

VCAM-1 has been implied in leukocyte recruitment it is possible that the anti-inflammatory effects of rFGF1 are mediated through reduced endothelial *VCAM-1* expression.

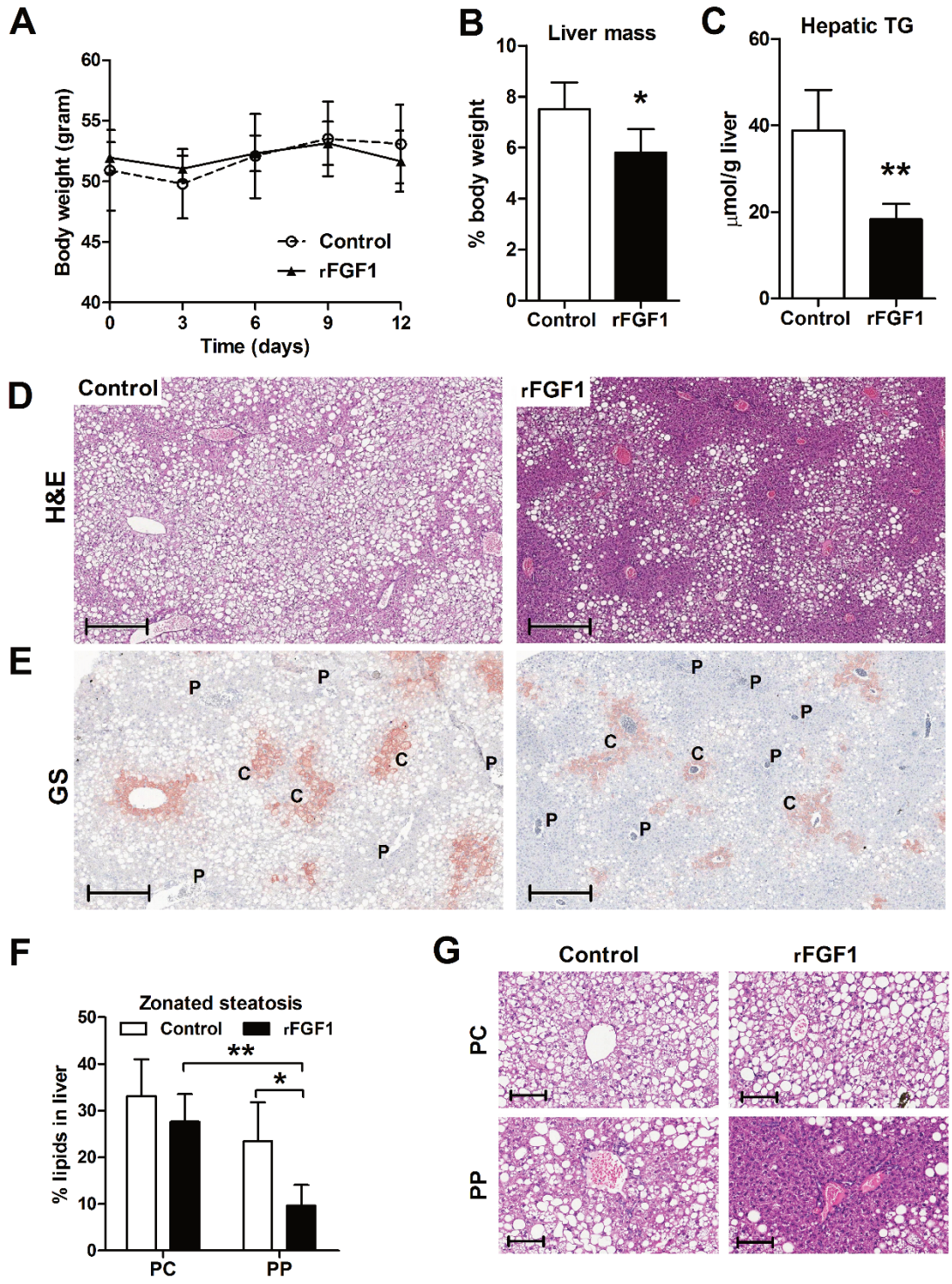

Fig. 1. rFGF1 reduces hepatic steatosis in ob/ob mice. (**A–C**) A 12-d rFGF1 treatment (0.5 mg/kg i.p. every 72 h) of ob/ob mice does not affect body weight (**A**) but does reduce liver mass (**B**) and hepatic triglyceride levels (**C**) (n = 6; unpaired t-test with Welch's correction). (**D** and **E**) Histological visualization of steatosis in serial liver sections stained with H&E (**D**) and the central vein marker GS (**E**) combined with H&E. C, central vein; P, portal area (Scale bar: 300 µm) (**F**) Quantitation of zonal distribution of steatosis in liver (n = 6 slides per group; two-

way ANOVA), PC, pericentral zone; PP, periportal zone (**G**) High magnification H&E-stained liver sections show reduced steatosis at the periportal zone in rFGF1 treated animals (Scale bar: 90μM). *P < 0.05, **P < 0.01

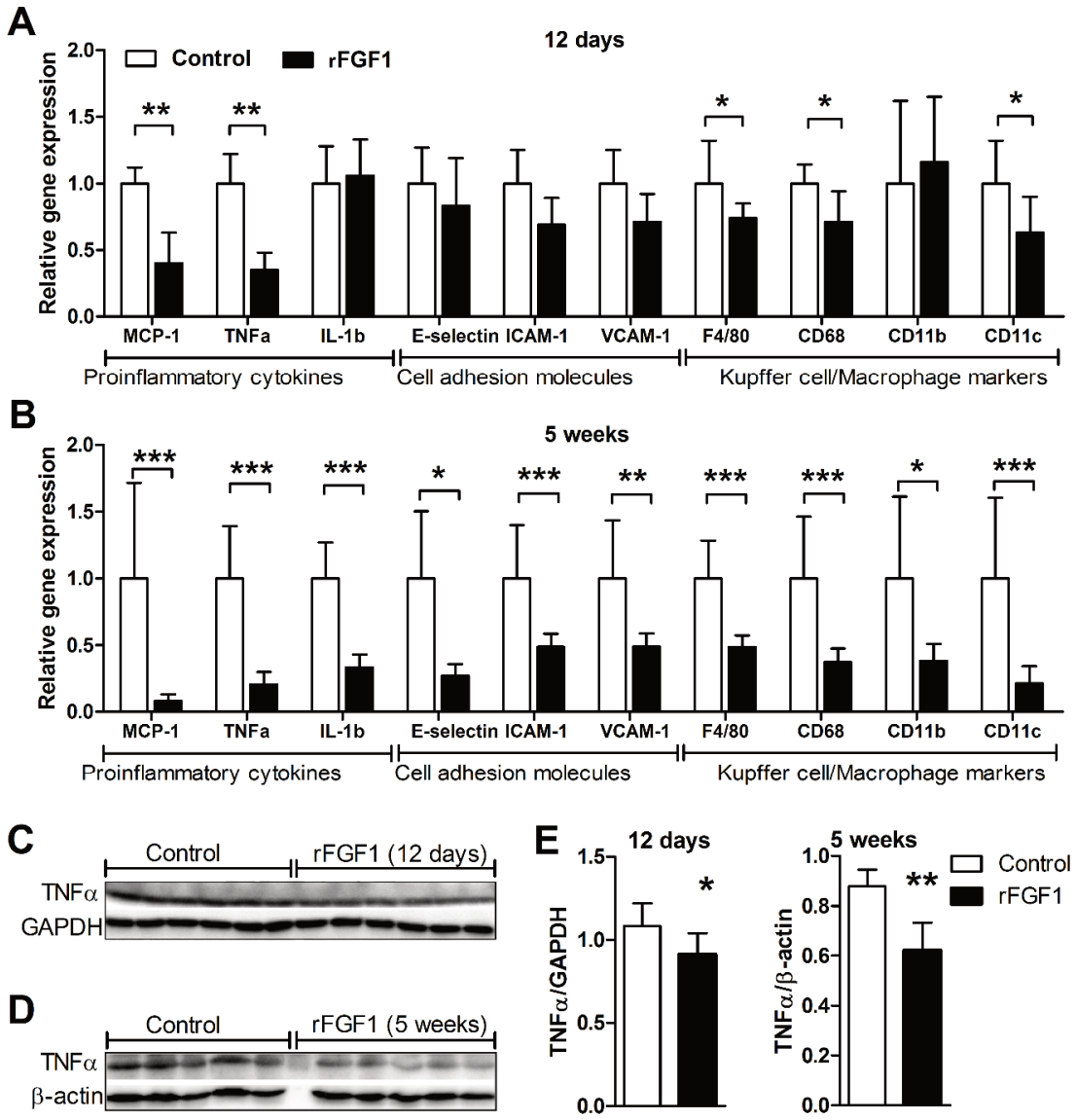

Fig. 2. rFGF1 suppresses hepatic inflammation in ob/ob mice. (**A** and **B**) Gene expression of inflammatory markers in livers of ob/ob mice treated with rFGF1 for 12 d (**A**) or for 5 wk (**B**). (**C**–**E**) Western blot analysis of TNF-α protein levels in the livers of rFGF1-treated ob/ob mice at 12 d (**C**) or 5wk (**D**). (**E**) Quantitation of (**C**) and (**D**). (n = 6–8; Mann–Whitney test). *P < 0.05, **P < 0.01, ***P <0.001.

The anti-steatotic effects of rFGF1 are absent in a choline-deficient model of steatosis. Steatosis results from an imbalance in hepatic lipid metabolism. Whereas hepatic fatty acid (FA) synthesis and triglyceride accumulation occur predominantly in the pericentral zone, FA oxidation (FAO) and secretion (VLDL production) are more associated with the periportal zone (11). Our observation that rFGF1 primarily reduces steatosis in the periportal zone thus suggested that rFGF1 improved hepatic lipid catabolism (*i.e.* oxidation and/or secretion). To further investigate how rFGF1 exerts its anti-steatotic effects, we used a choline-deficient L-amino acid defined (CDAA) diet, a commonly used rodent model for steatosis (10). In contrast

to *ob/ob* mice and diet-induced obesity (DIO) models of steatosis, which have increased hepatic lipid accumulation due to excessive food intake, choline-deficiency causes a defective hepatic lipid catabolism resulting in steatosis in the absence of obesity or insulin resistance (10).

Mice were challenged with the CDAA or control choline-supplemented (CSAA) diet for 3 or 6 wks and the preventive effect of rFGF1 (0.5 mg/kg i.p. every 3 days) on the development of NAFLD/NASH was monitored. Body weights and white adipose mass of both control and rFGF1-treated mice increased at similar rates and were not significantly different as compared to the dietary control group (**Fig. 4*A*, *B***). Liver mass, as a percentage of body weight, increased from ~4% to ~6% in the first 3 wks but remained stable at 6 wks (**Fig. 4*C***). As expected, hepatic TG levels in the CDAA-challenged mice progressively increased over time as compared to the CSAA control mice but no effect of rFGF1 was observed on either liver mass or hepatic TG (**Fig. 4*C, D***). These findings were supported by histological examination using H&E and Oil red O staining (**Fig. 4*E,F***; **Fig. S3**and **S4**). GS staining further indicated a clear periportal localization of the steatosis in the CDAA model similar to what has previously been described (**Fig. 4*G***) (12). Together, these results suggest that the anti-steatotic effects of rFGF1 are dependent on the catabolic processes that are defective in the CDAA model.

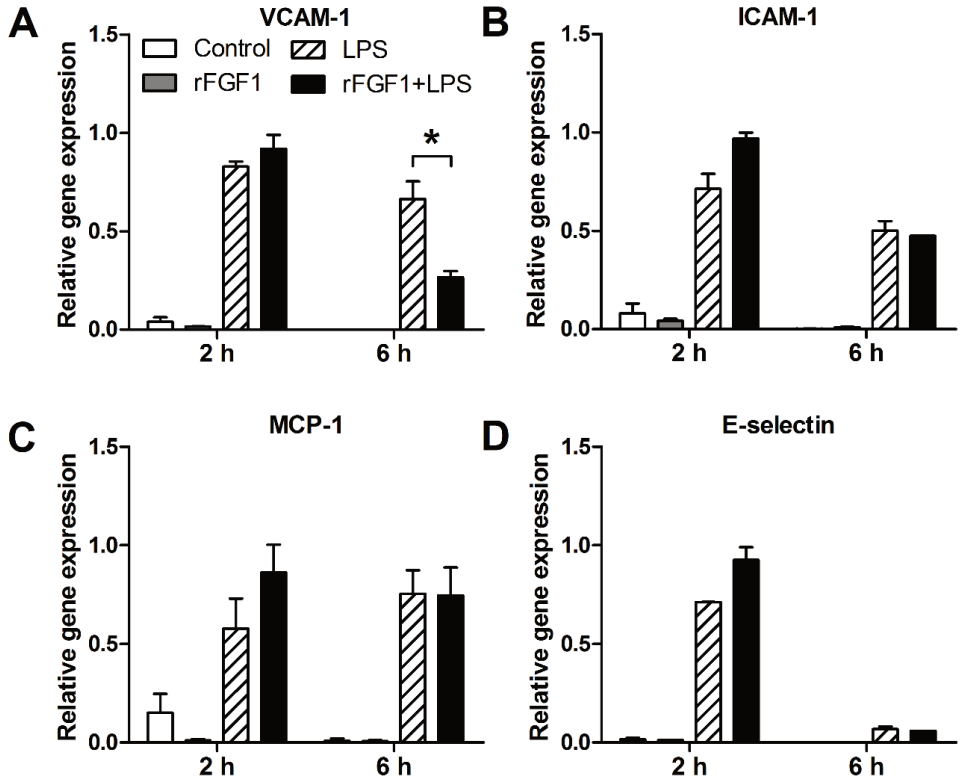

Fig. 3. Effect of rFGF1 on activation of HUVEC endothelial cells. The expression of *VCAM-1* (**A**), *ICAM-1* (**B**), *MCP-1* (**C**), and *E-selectin* (**D**) in HUVECs after activation by LPS (n = 3; *P < 0.05; Mann–Whitney test).

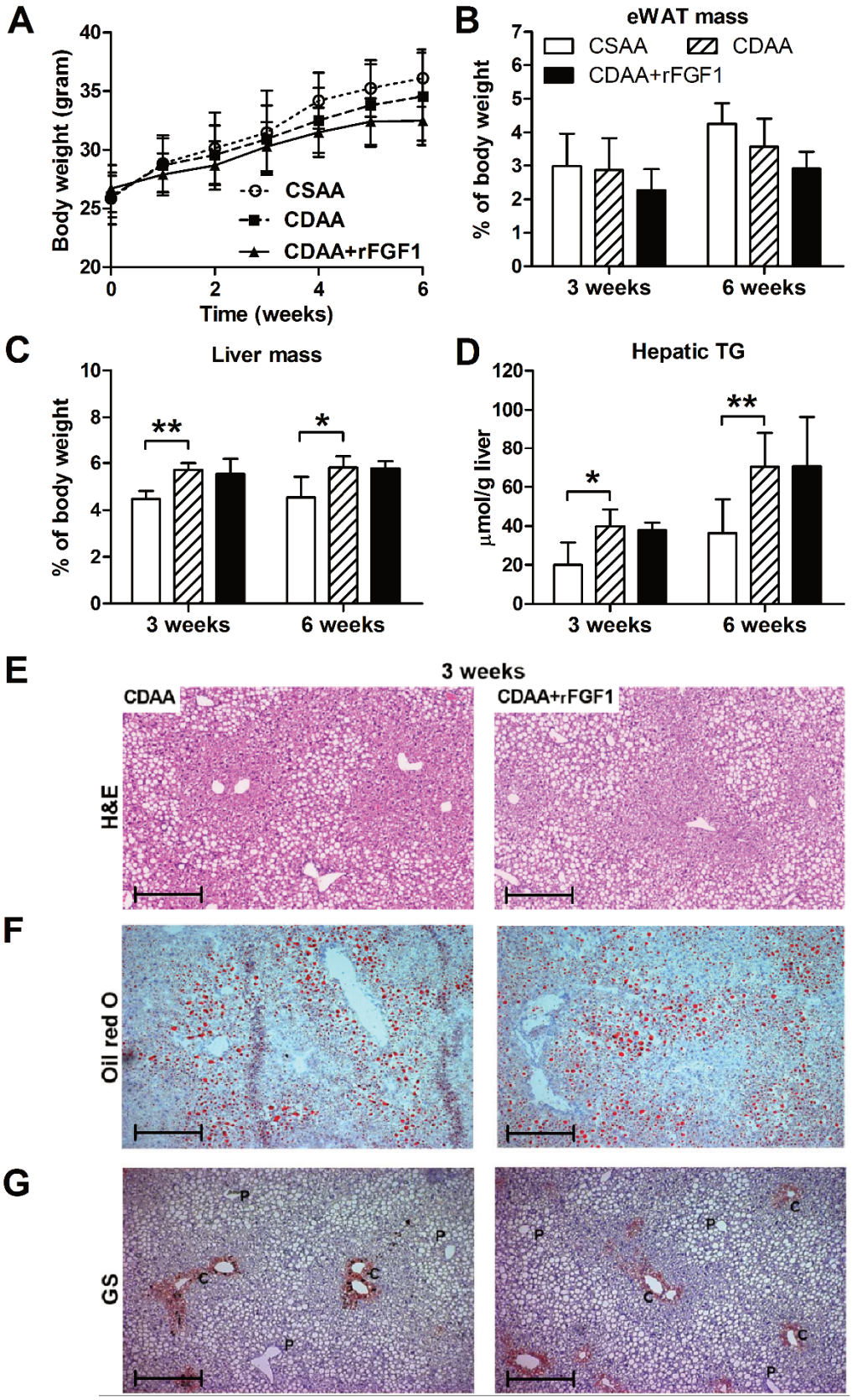

Fig. 4. rFGF1 does not reduce steatosis in mice with a dietary choline deficiency. (**A–D**) rFGF1 does not affect body weight (**A**), epididymal white adipose tissue (eWAT) mass (**B**), liver mass (**C**), or hepatic triglyceride (TG) levels (**D**) in mice challenged for 3 or 6 wk with a CDAA or on a control CSAA diet (n = 8 or 10 mice per group;

one-way ANOVA). (**E–G**) Histological visualization of steatosis in serial liver sections after a 3-wk CDAA challenge, with (Left) or without (Right) rFGF1, stained with H&E (**E**), Oil red O (**F**), or the central vein marker GS combined with H&E (**G**). C, central vein; P, portal vein. (Scale bar: 300 μm). *P < 0.05, **P < 0.01.

rFGF1 suppresses hepatic inflammation independent of its anti-steatotic effects. Since rFGF1 did not affect steatosis in the CDAA model, this model allowed us to investigate whether the anti-inflammatory properties of rFGF1 are dependent on its anti-steatotic properties. After a 3 wk CDAA challenge, significant reductions in the mRNA expression of *MCP-1*, *TNFα*, *ICAM-1*, *VCAM-1* and *CD11c* were observed in rFGF1 treated mice as compared with the CDAA control mice (**Fig. 5*A***). In addition, a trend towards decreased expression was observed for *IL-1β* and *E-selectin* in rFGF1-treated mice. Reduced hepatic inflammation was further confirmed by histopathological and protein analysis, indicating a reduction in the number of inflammatory foci in the liver (**Fig 5*B***, **Table S2** and reduced levels of MCP-1 protein (**Fig. 5*C***). These data show that rFGF1 exerts its anti-inflammatory effect in the liver independently from its anti-steatotic effect. After a 6 wk CDAA challenge, mRNA expression of inflammatory markers however, were no longer reduced by rFGF1-treatment or even increased in the case of E-selectin (**Fig. S5**). In addition, no effect of rFGF1 on anti-inflammatory M2 marker expression was observed (**Fig. S1*C, D***). Histopathological analysis further indicated that lobular inflammation was increased in the rFGF1-treated mice as compared to the CDAA control mice (**Table S3**).

Interestingly, rFGF1 also prevented the increase in plasma levels of ALT activity, a marker for liver damage, after a 3 wk CDAA challenge and a similar trend was seen after 6 wks (**Fig. 5*D*, Fig. S5**). rFGF1 may thus have hepato-protective properties beyond its anti-steatotic and anti-inflammatory properties. In line with this finding, it has previously been reported that FGF1/FGF2 double knockout mice exhibit increased levels of ALT after tetrachloride-induced hepatic injury (13). Together, our results show that in the CDAA model, rFGF1 can prevent liver damage as reflected by plasma ALT and that it can delay but not prevent hepatic inflammation.

rFGF1 does not induce hepatic fibrosis or proliferation. Potential adverse effects of FGFs are fibrosis and proliferation. Previous studies have implied a role for FGF1 in promoting hepatic fibrosis. Increased expression of *FGF1/FGFRc* was observed in a rat model of experimental pulmonary fibrosis and in patients with idiopathic pulmonary fibrosis, respectively (14,15). Conversely, loss of FGF1 and -2 in mice resulted in decreased liver fibrosis upon exposure to carbon tetrachloride (13). To assess the effect of rFGF1 on the development of hepatic fibrosis, liver samples from 5 wk treated *ob/ob* mice were analyzed for the expression of fibrogenic maker genes. The expression of *TGF-β1*, which has been shown to accelerate liver fibrogenesis by promoting hepatic stellate cell (HSC) transformation and activation of the expression of extracellular matrix genes (16), was significantly reduced in rFGF1-treated *ob/ob* mice as compared to control mice (**Fig. 6*A***). The expression of *collagen-α1*, *αSMA* and *TIMP-1*, however, was not significantly different. Also, no significant differences in the expression of fibrogenic genes or collagen deposition were observed between control and rFGF1-treated mice after a 3 or 6 wk CDAA challenge, respectively (**Fig. 6*B-D,* Fig. S6**). Finally, we observed a significant reduction in the expression of the proliferation

marker *Ki-67* by rFGF1 after a 3 wk CDAA challenge whereas no difference was observed after 6 wks (**Fig. 6*E,F***). These findings were supported by histopathological analyses (**Table S4**). Together, these results suggest that rFGF1 has no adverse effects on hepatic fibrosis or proliferation.

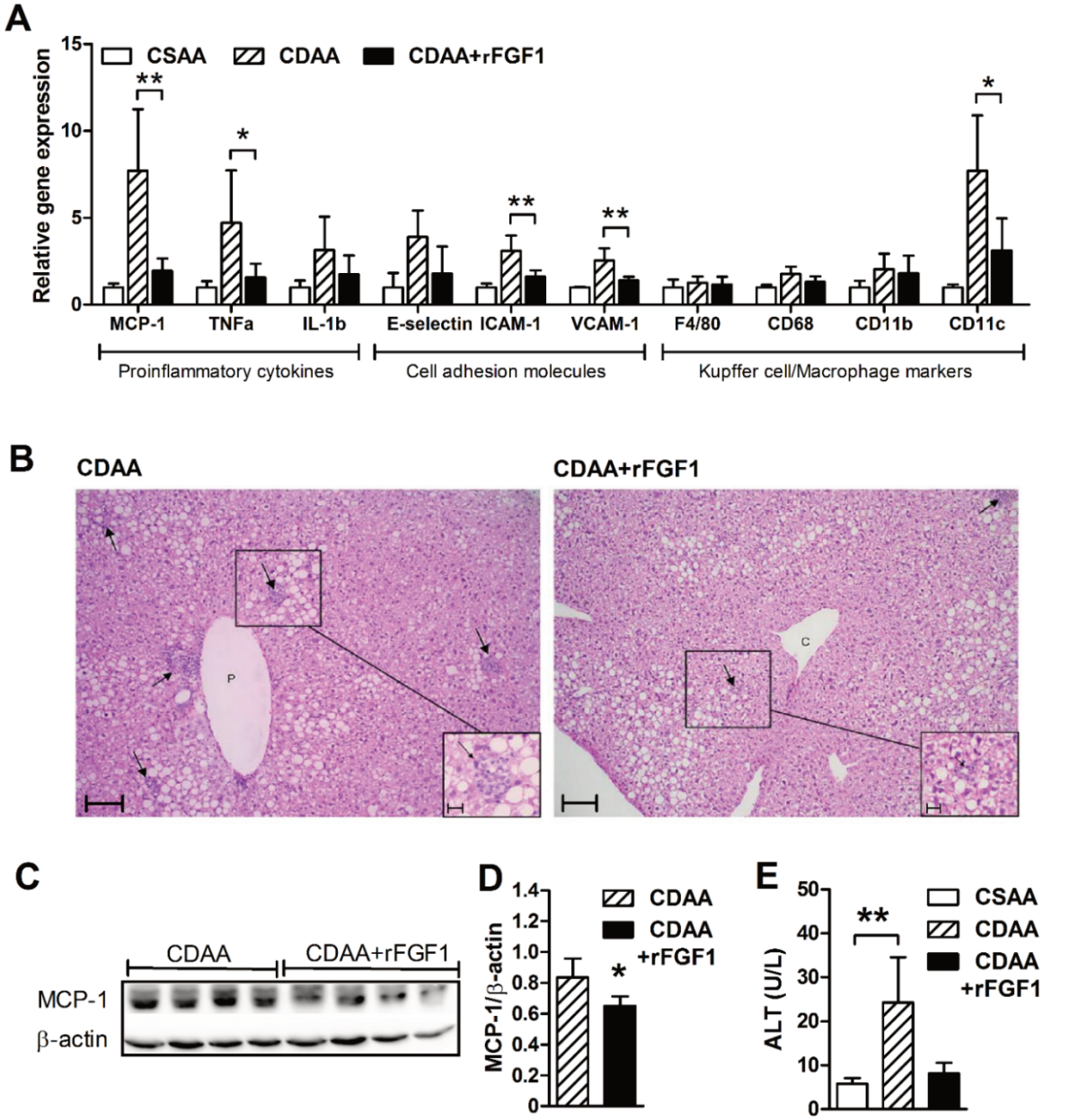

Fig. 5. rFGF1 suppresses hepatic inflammation in mice with a dietary choline deficiency. (**A**) Effect of rFGF1 on the expression of inflammatory genes in the livers of mice challenged for 3 wk with a CDAA diet or on a CSAA diet (n = 8 or 10; one-way ANOVA). (**B**) Histological visualization of inflammation in H&E-stained liver sections. Aggregations of lymphocytes, indicating lobular inflammation, are indicated by arrows. C, central vein; P, portal area. (**C**) Western blot analysis of MCP-1 protein levels. (**D**) Quantitation of (**C**) (unpaired t test with Welch's correction). (**E**) ALT activity (n = 3 or 5; one-way ANOVA). *P < 0.05, **P < 0.01.

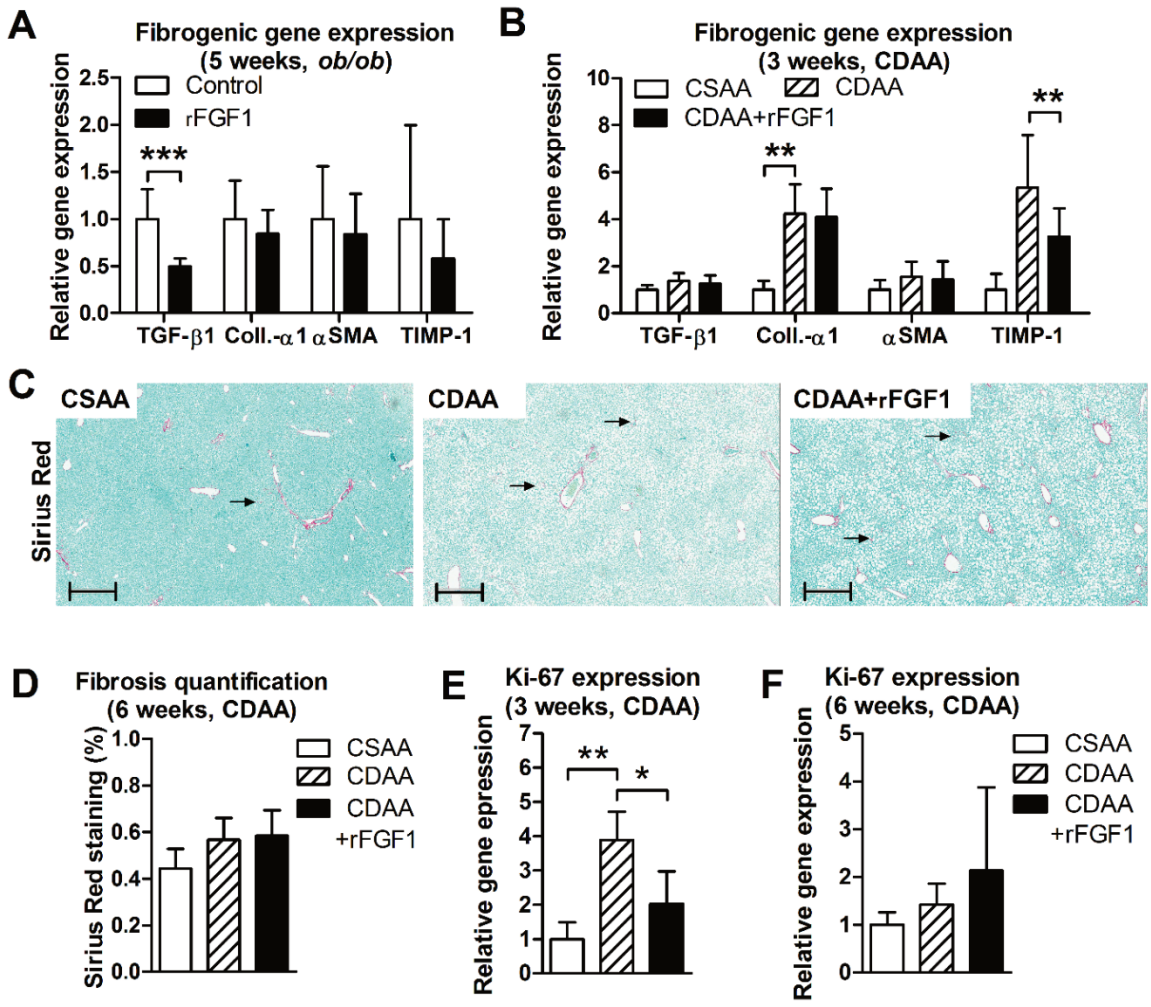

Fig. 6. FGF1 does not promote hepatic fibrosis and proliferation in ob/ob mice or in choline-deficient mice. (**A** and **B**) Fibrogenic gene expression in ob/ob mice treated for 5 wk with rFGF1 (n = 6 or 8; Mann–Whitney test) (**A**) and in mice challenged for 3 wk (n = 5 or 6) with a CDAA diet (n = 8–10) or on a CSAA (n = 5 or 6; one-way ANOVA) (**B**). (**C**) Histological visualization of fibrosis in liver sections stained with Sirius red from mice challenged for 6 wk with a CSAA diet or on a CDAA diet with or without rFGF1. Arrows indicate pericentral and hepatocyte collagen deposition (Scale bars: 500 μm.) (**D**) Quantitation of fibrosis in liver sections from mice challenged for 6 wk with a CSAA diet or on a CDAA diet with or without rFGF1 (n = 5 slides per group; one-way ANOVA). (**E** and **F**) Expression of *Ki-67* in mice fed the CDAA diet for 3 wk (E) or 6 wk (F) (n = 5 or 6). *P < 0.05, **P < 0.01, ***P <0.001.

Discussion

Here we show that pharmacological administration of rFGF1 effectively improves obesity-related steatosis, hepatic inflammation and damage. Our findings further suggest that these effects are at least partially independent, as the anti-inflammatory effects were observed both in the presence and absence of anti-steatotic effects.

While no pharmacological treatment has currently been approved for NAFLD/NASH, insulin sensitizers and anti-oxidative treatment strategies with vitamin E are among the best-established approaches (1). Both of these approaches, however, have long-term safety issues and there is only limited evidence of improvement in cirrhotic patients (1,17). Whereas vitamin E treatment is associated with increased mortality, TZDs have been associated with various

adverse effects including weight gain, fluid retention and osteoporosis, complicating their clinical use (4, 18). In addition, TZDs are contra-indicated in patients with symptomatic chronic heart failure (19). Current strategies for novel PPARγ-based treatments are therefore directed at developing selective receptor modulators (SRMs) with reduced adverse effects or at activation of selective downstream targets (20).

Recently, we have identified FGF1 as a target of nuclear receptor PPARγ in visceral adipose tissue and as a critical factor in adipose function, insulin resistance and the development of type 2 diabetes (8,9). When challenged with a high-fat diet, mice lacking FGF1 display aberrant adipose expansion, characterized by reduced angiogenesis, increased adipose-inflammation and -fibrosis and resulting in ectopic fat accumulation in the liver and in insulin resistance (8). Conversely, pharmacological administration of rFGF1 improved hyperglycemia, insulin sensitivity and steatosis in mouse models of obesity (9).

Two other members of the FGF family, the endocrine hormones FGF15/19 and FGF21 have also been shown to improve hyperglycemia, insulin resistance and steatosis (21). The effects of FGF15/19 are mediated directly through activation of FGF receptor 4 (FGFR4) and its co-receptor β-klotho in the liver (19,20). FGF15/19 is produced in the ileum, where its expression is controlled by the bile acid activated nuclear receptor FXR, and is subsequently secreted into the circulation (22,23). In the liver, FGF15/19 suppresses bile acid synthesis and gluconeogenesis (22,24,25). Although we have not observed effects of FGF1 on bile acid homeostasis, it is possible that some of its metabolic effects are mediated directly through hepatic FGFR4 activation, since FGF1 acts as a universal ligand for all FGFRs. In contrast to FGF15/19, the glycemic effects of FGF1 and FGF21 are dependent on FGFR1 activation in adipose tissue (9, 26). For FGF21, it has further been demonstrated that it can alleviate endoplasmic reticulum (ER) stress-induced hepatic steatosis by acting as a metabolic effector of the unfolded protein response (27). Whether these effects are directly mediated through FGFR activation in the liver and whether FGF1 and FGF15/19 are acting through the same pathway is not known.

In contrast to *ob/ob* mice and DIO models of steatosis, we did not observe an improvement in steatosis in the choline-deficient model. The difference in etiology of the steatosis in these models gives a clue in the mechanism of action of FGF1. Whereas *ob/ob* mice and DIO mice have increased hepatic lipid accumulation due to excessive food intake, a choline-deficiency causes a defective hepatic β-oxidation and very-low-density lipoprotein (VLDL) production resulting in steatosis in the absence of obesity or insulin resistance (10,28). These differences in the pathophysiology of steatosis were also clearly reflected in the zonal distribution of lipids in these models. Whereas steatosis in *ob/ob* mice was primarily located in the pericentral region, in the CDAA model this was mainly present in the periportal region. Hepatic zonation plays an important role in the segregation of the different metabolic pathways in the liver (11,29). Hepatic fatty acid (FA) synthesis and triglyceride accumulation occur predominantly in the pericentral zone, whereas catabolic processes such as FA oxidation (FAO) and secretion (VLDL production) on the other hand are more associated with the periportal zone (11). Our observation that reduction of steatosis by rFGF1 is limited to the periportal zone thus suggests that rFGF1 acts by improving hepatic lipid catabolism (*i.e.* oxidation and/or secretion).

Hepatic lipid metabolism and inflammation are tightly linked processes and both are known to exacerbate insulin resistance (30). The accumulation of toxic lipid species and their metabolites, such as saturated free fatty acids (FFAs), free cholesterol and the sphingolipid ceramide, has been shown to exert an inflammatory response through activation of Bax protein translocation which in turn triggers lysosomal and mitochondrial permeabilization, ROS production and apoptosis (31). This process is called lipotoxicity and promotes activation of Kupffer cells (KCs), specialized macrophages in the liver, and results in exacerbation of insulin resistance and progression of NASH (32). Our results show that rFGF1 effectively suppresses hepatic inflammation both in *ob/ob* mice and choline deficient mice as indicated by significant reductions in the expression of the pro-inflammatory M1 markers *MCP-1* and *TNFα*. Interestingly, the anti-inflammatory effect of rFGF1 became more pronounced with prolonged (5 wks) treatment in *ob/ob* mice, as evidenced by further suppression of M1 markers, but also of cell adhesion markers (*E-selectin, VCAM-1, ICAM-1*) and macrophage/KC markers (*F4/80, CD68, CD11b and CD11c*). Whereas rFGF1 also suppressed hepatic inflammation after a 3 wk challenge with a choline-deficient diet, this effect was no longer observed at 6 wks. It is possible, however, that the anti-inflammatory effect of rFGF1 is only achieved in the presence of relatively low levels of hepatic lipids (*e.g.* 3 wk CDAA) and that when levels of hepatic lipids become progressively higher (*e.g.* 6 wk CDAA), the anti-inflammatory effect of rFGF1 is mitigated due to lipotoxicity.

Our *in vitro* data suggests that rFGF1 does not suppress inflammation through a direct effect on hepatocytes or through macrophage activation. We did, however, find a strong suppression of *VCAM-1* expression in HUVEC endothelial cells. Sinusoidal endothelial cells play a major role in hepatic inflammation through their involvement in adhesion molecule-mediated recruitment of leukocytes (33). It was shown previously that FGF1 suppresses trans-endothelial leukocyte migration by reducing expression of several endothelial adhesion molecules, including *VCAM-1* (34). Endothelial cells in normal liver express little or no *VCAM-1*, whereas it is highly induced during conditions of steatohepatitis (35). Based on these findings we speculate that rFGF1 *in vivo* decreases leukocyte recruitment by reducing endothelial *VCAM-1* and thereby suppresses hepatic inflammation.

Together, our findings show that FGF1 has therapeutic potential in the treatment of NAFLD and NASH. As FGF1 is situated downstream of PPARγ, it is likely that therapeutic targeting of FGF1 will eliminate some of the adverse effects associated with TZDs that are mediated through direct activation of PPARγ.

Experimental Procedures

Animals. Mice were housed and handled according to institutional guidelines complying with Dutch legislation. All experiments were approved by the Ethical Committee for Animal Experiments, University of Groningen, The Netherlands. Animals used in this study were male wild-type and *ob/ob* mice on a C57Bl/6J genetic background (Charles River, France), between 8-12 wks of age. Animals were housed in a light- and temperature-controlled facility (lights on from 7 a.m. to 7 p.m., 21 °C). All mice received a standard laboratory chow (RMH-B; Hope Farms, Woerden, The Netherlands) and acidified water *ad libitum*.

Animal experiments. Choline-deficiency was induced by a 3 or 6 wk challenge with a choline-deficient L-amino acid defined (CDAA) diet (CDAA, #518753) or a choline-sufficient control diet (CSAA, #518754) (Dyets inc., PA, USA). Mice were treated with vehicle (PBS) or rFGF1 (0.5 mg/kg, Prospec, Rehovot, Israel) by intraperitoneal (i.p.) injection starting 3 days before the dietary intervention and then every 72 h for 3 or 6 wks. Mice were euthanized by cardiac puncture after anesthesia with isoflurane. Terminal blood samples were collected in EDTA-coated tubes. Tissues were collected and frozen in liquid nitrogen or processed for histology. Hepatic lipids were extracted according to Bligh & Dyer. TGs were determined using *Trig/GB* kit (Roche #11877771) and absorption at 540 nm. Plasma was obtained by centrifugation at 6,000 rpm for 10 min and used for determination of alanine transaminase (ALT) activity using the spinreact GOT-GPT kit (# 1002500, Girona, Spain).

Protein analysis. For immunoblot analysis, total liver was homogenized in liquid nitrogen and whole-cell lysates were prepared in RIPA lysis buffer (SLB: Tris-HCL pH=8, 138 mM NaCl, 1% (v/v) Nonidet P-40 , mM KCL 2.7, 1 mM $MgCl_2$, 5% (v/v) Glycerol , 5 mM EDTA, 1 mM Na_3VO_4, 20 mM NaF, 1mM DTT and protease inhibitor) and protein concentrations were determined using the BCA Protein Assay kit (Thermo Scientific, IL, USA). Protein samples were subjected to SDS-PAGE (15% gels) and transferred to nitrocellulose using Trans-Blot® Turbo™ transfer system (Bio-Rad). After blocking for one hr at room temperature (RT) in PBS containing 0.1% (v/v) Tween and 2% (w/v) milk powder, membranes were o/n incubated with primary antibodies at 4°C. Antibodies used in this study are: anti-TNFα (rabbit polyclonal [52B83], ab6671, Abcam, UK), anti-MCP1 (mouse monoclonal, AM32136PU-N, Acris, DE), anti-β-Actin (rabbit polyclonal, a2066, Sigma) and anti-GAPDH (mouse monoclonal, CB1001-500UG, Calbiochem). Antibodies were detected by incubating the blot with horseradish peroxidase (HRP)-conjugated donkey anti-rabbit (Life science, NA934) or rabbit anti-mouse (Dako, p0260) IgG for 1h at RT. Image Lab software (Bio-Rad) was used for densitometry.

Histological analysis and immunohistochemistry. For microscopic examination, tissues were fixed in 4% (w/v) phosphate-buffered formalin, embedded in paraffin, sectioned at 4 μm, and stained with haematoxylin and eosin (H&E). Liver fibrosis was assessed by Sirius red staining. Liver steatosis was visualized by Oil red O staining of liver cryosections. For determination of zonation, GS staining was used for central vein localization (36). Briefly, sections were deparaffinized in xylene and rehydrated in a series of graded alcohol washing steps. Antigen retrieval was conducted by mildly boiling of sections in 1 mM EDTA solution, pH 8.0 for 15 minutes. Endogenous HRP activity was blocked in 0.3% (v/v) H_2O_2, 10% (v/v) normal goat serum in 1% (w/v) BSA PBS solution was used to block non-specific binding prior to antibody incubation. Anti-glutamine synthetase (mouse IgG_{2a}, 610518, BD Biosciences, USA) primary antibody was o/n incubated at 4°C, then washed with PBS followed by incubation with HRP-conjugated goat anti-mouse IgG (Invitrogen, R40101), incubation for 1 hour at RT. AEC reagent containing 0.3% (v/v) H_2O_2 was used for visualization.

Assessment of hepatic steatosis and steatohepatitis was performed in an unbiased manner by two board certified pathologists. Hepatic steatosis and inflammation were graded in H&E stained liver sections by using an adapted version of the NAS scoring system for NAFLD developed by Kleiner et al. (37). For quantitation of steatosis, H&E- and glutamine synthetase

(GS)-stained sections (6 slides for each group) were randomly selected. Next, 3 to 4 pericentral or periportal areas on each section were selected and quantified for steatosis using ImageJ.

Gene expression analysis. Total RNA was isolated from the liver using Tri reagent (Life Technologies, USA) and reverse transcribed into cDNA using M-MLV, random primers and dNTPs according to standard procedures. For quantitative PCR (qPCR), cDNA was amplified using Hi-ROX SensiMix™ SYBR green (Bioline, London, UK) and StepOnePlus™ Real-Time PCR System (Applied Biosystems, CA, USA). Primers used for qPCR are listed in Table S5. U36B4 was used as the house-keeping gene in all PCR analyses and the ΔΔCt method was used for quantification.

Isolation of primary rat hepatocytes and cell culture. Rat primary hepatocytes were isolated from Wistar rats based on the two-step collagenase perfusion method (38). Cells were seeded into collagen-coated plates and o/n recovered in dexamethasone-containing William's E complete medium. Prior to experiments, the medium was replaced by dexamethasone-free William's E complete medium supplemented with 5% (v/v) charcoal-stripped serum + 1% (v/v) penicillin streptomycin (p/s). Then, cells were pre-incubated with 100 ng/ml rFGF1 or PBS for 2 h. Subsequently, an acute inflammatory response was elicited using mTNFα (20 ng/ml) and hIL-1β (10 ng/ml). RAW264.7 cells were cultured in RPMI 1640 medium supplemented with 10% (v/v) FBS and 1% (v/v) p/s and maintained at 37°C under 5% CO_2. Human umbilical vein endothelial cells (HUVECs) (Lonza, CC2519) were cultured in EGM-2 medium (Lonza) on 1% (w/v) gelatin-coated plates. For activation, cells were treated with 100 ng/ml lipopolysaccharide (Sigma) after 2 h rFGF1 pre-incubation. RNA samples were collected at different time points to assess the expression of inflammatory marker genes.

Statistical Analysis. All values are given as means ± SD. The two-tailed unpaired student's t-test with Welch's correction, nonparametric Mann-Whitney test, one-way or two-way ANOVA analysis with Holm-Sidak's multiple comparison test were used for statistical analysis. Significance was indicated as $*P < 0.05$, $**P < 0.01$, $***P < 0.001$.

Author contributions: W.L., D.S., T.v.Z., M.D., R.M.E. and J.W.J. designed research; W.L., D.S., A.J., L.H., T.v.Z. and J.W.J performed research; W.L., D.S., V.J.M.N., A.B., H.J.V., M.D., R.M.E., T.v.Z. and J.W.J. analyzed data; W.L., D.S., T.v.Z. and J.W.J. wrote the paper.

Acknowledgments
We thank our colleagues for critical reading of the manuscript. Prof. Annette Gouw for help and suggestions on histological analysis. J.W.J. is supported by grants from The Netherlands Organization for Scientific Research (VIDI grant 016.126.338), the Dutch Digestive Foundation (grant WO 11-67) and the Dutch Diabetes Foundation (grant 2012.00.1537).

Supporting information

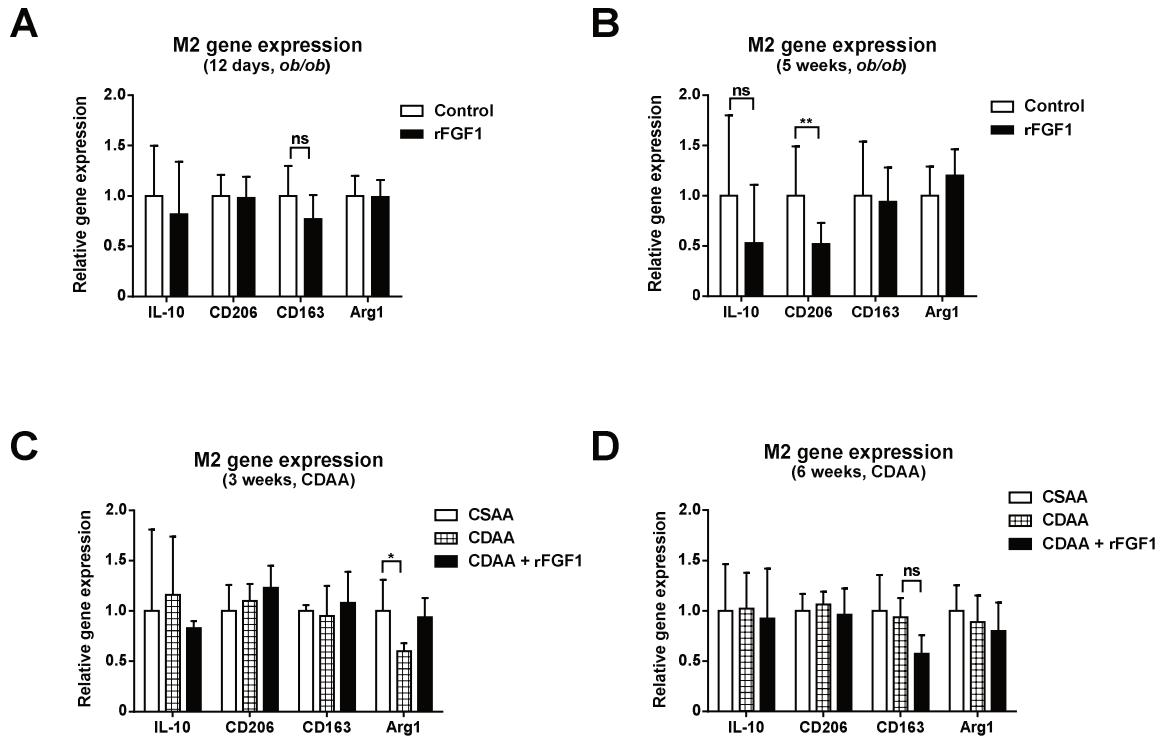

Fig. S1. Hepatic expression of M2 markers in ob/ob mice treated with rFGF1 for (**A**) 12 days (n=6) and (**B**) 5 weeks (n=8), (**p<0.01, Mann-Whitney test); Hepatic expression of M2 markers in C57BL/6 mice fed with a CDAA diet for (**C**) 3 weeks (n=5) and (**D**) 6 weeks (n=5), *P<0.05, vs. CSAA group (one-way ANOVA).

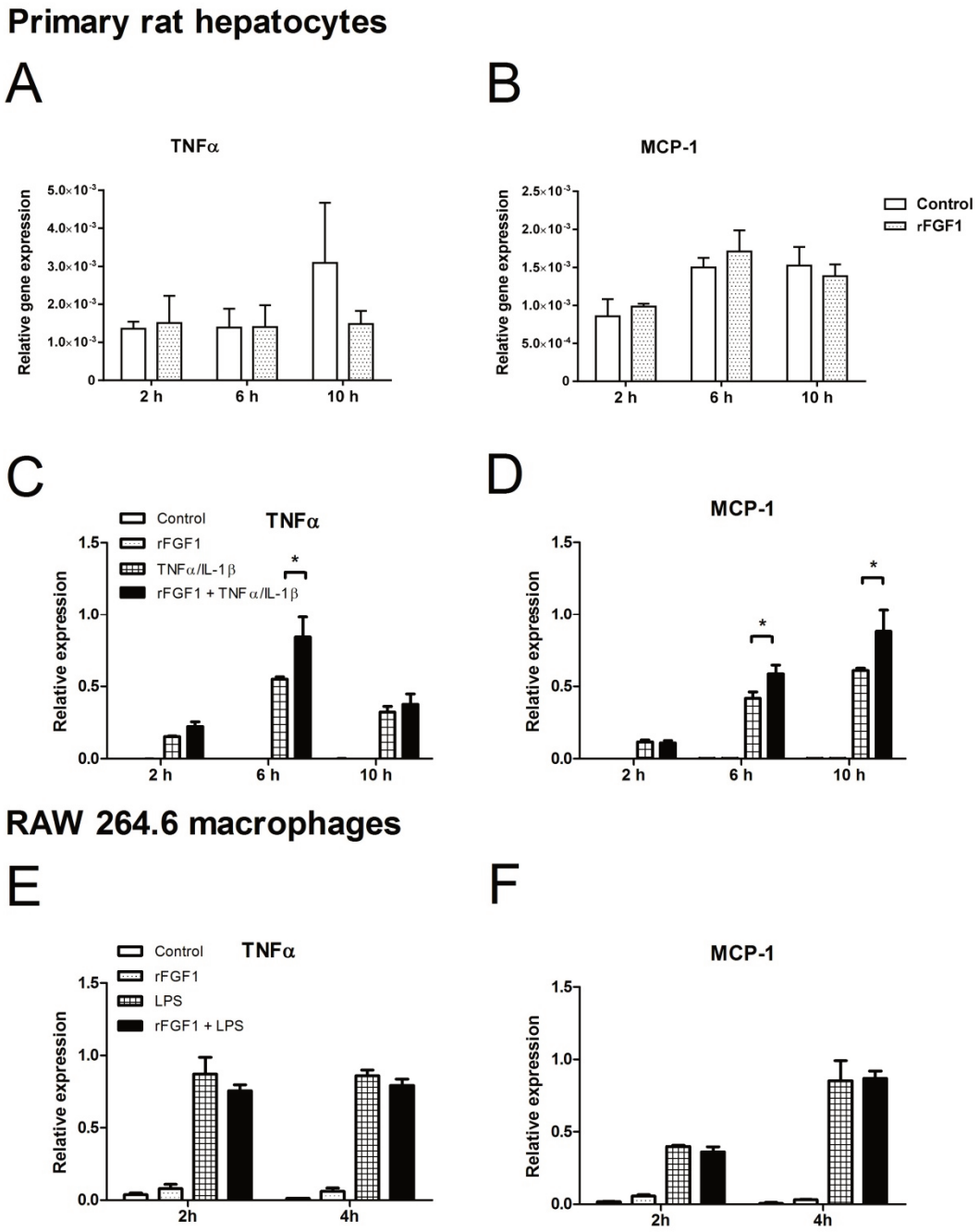

Fig. S2. Effect of rFGF1 on the mRNA expression of (***A***) TNFα and (***B***) MCP-1 in unstimulated primary hepatocytes and stimulated with of TNFα and IL-1β (***C,D***). The expression of *(**E**) MCP-1* and *(**F**)* T*NFα* in murine RAW267.4 macrophage cells at different time points after rFGF1 treatment and activation by LPS, (n=3, nonparametric Mann-Whitney test); **P*<0.01.

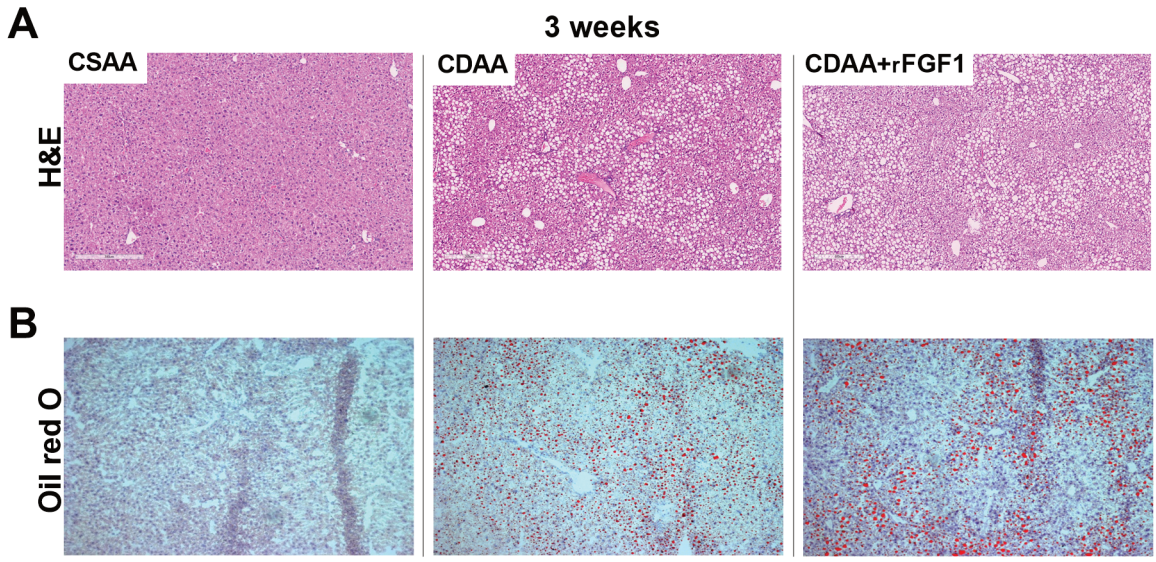

Fig. S3. Effect of rFGF1 on liver (**A**) histology (H&E) and (**B**) lipid accumulation (Oil Red O) of male C57BL/6 mice (n = 8-10) challenged for 3 weeks with a choline deficient diet, (CDAA = choline deficient L-amino acid defined) or a choline supplemented control diet (CSAA = choline supplemented L-amino acid defined), Representative images are shown, (scale bar = 300µm).

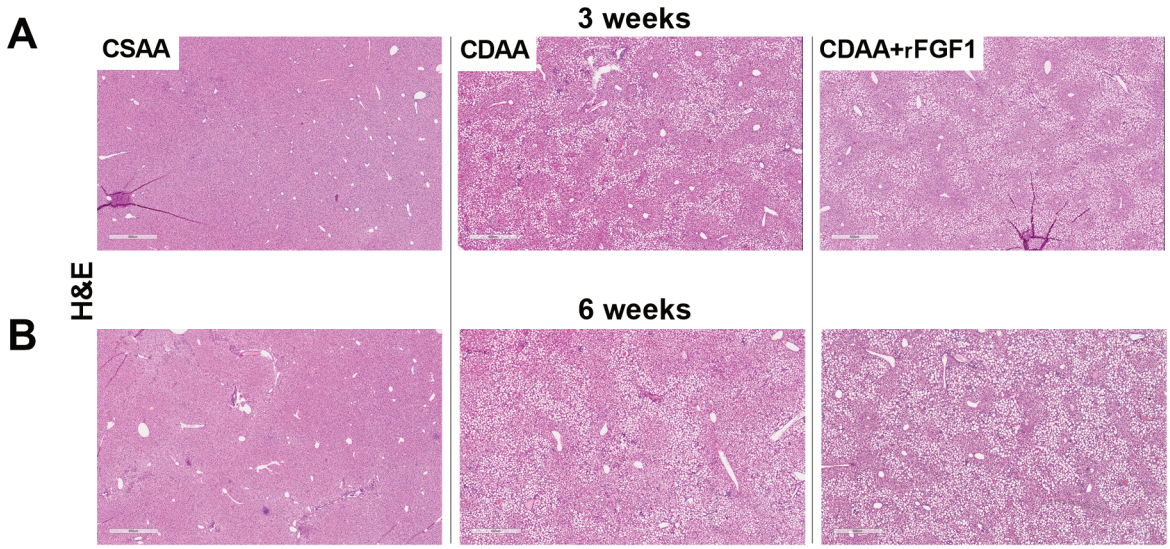

Fig. S4. Effect of rFGF1 on liver histology (H&E) of male C57BL/6 mice (n = 8-10) challenged for (**A**) 3 weeks and (**B**) 6 weeks with a choline deficient diet, (CDAA = choline deficient L-amino acid defined) or a choline supplemented control diet (CSAA = choline supplemented L-amino acid defined), Representative images are shown, (scale bar = 600µm).

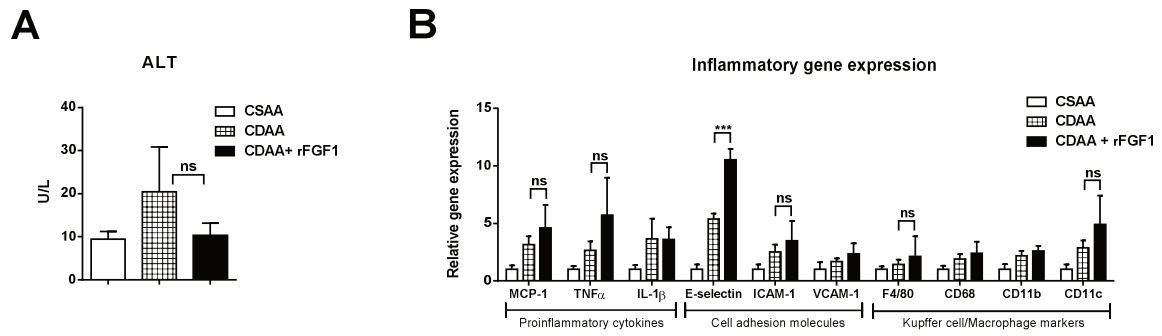

Fig. S5. Effect of rFGF1 on (**A**) plasma ALT levels and (**B**) hepatic gene expression of inflammatory markers in livers of male C57BL/6 mice (n = 8-10) challenged for 6 weeks with a choline deficient diet, (CDAA = choline deficient L-amino acid defined) or a choline supplemented control diet (CSAA = choline supplemented L-amino acid defined), (n=5, one-way ANOVA).

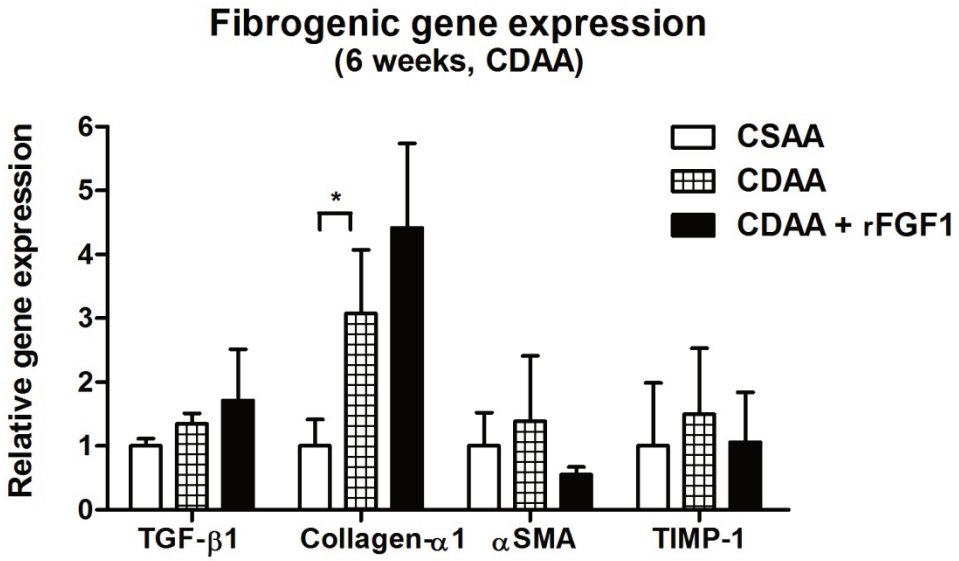

Fig. S6. Fibrogenic gene expression after 6 weeks of choline-deficient diet (CDAA) or choline-supplemented control diet (CSAA). (one-way ANOVA).

Tables

Table S1. Histopathologic analysis of effects of rFGF1 on hepatic inflammation in *ob/ob* mice.

	Control		FGF1-treated	
Lobular inflammation*	0.5 (1) 1 (4) 1 (7) 0.5 (2) 1 (7) 0.5 (2)		0.5 (3) 0.5 (3) 0 0.5 (3) 1 (4) 1 (4)	
	Average	**0.75**	**Average**	**0.58**
Ballooning#	1.5 1.5 1.5 2 1.5 1.5		1 2 1 1 1 1.5	
	Average	**1.58**	**Average**	**1.25**

Table S1. Histopathologic evaluation of hepatic inflammation in control and FGF1-treated (12 days) *ob/ob* mice. Lobular inflammation and hepatocyte ballooning scores for each mouse are listed in the table, and the average value of each parameter is indicated under the dash line. *Lobular inflammation is scored from 0 to 3, 0=none; 1=<2 average inflammatory foci per 200x field; 2=2-4 foci; 3=>4 foci; number in ( ) indicates total foci of 5 random fields at 200x. #Ballooning score (0-2),0=none; 1=few balloon cells; 2=many cells/prominent ballooning.

Table S2. Histopathologic analysis of effects of rFGF1 (3 weeks) on hepatic inflammation in choline-deficient mice.

	CSAA	CDAA	CDAA + rFGF1
Lobular inflammation	0 0 1(4) 0	1 (6) 0.5 (3) 2 (11) 1 (5) 2 (14)	0.5 (3) 1 (5) 1 (6) 0.5 (3) 0
	Average 0.25	**Average 1.3**	**Average 0.6**
Ballooning	0 0 0 0	1 1 1 1.5 1	1 1 1 1 0
	Average 0	**Average 1.1**	**Average 0.8**

Table S2. Histopathologic evaluation of the effect of rFGF1 on hepatic inflammation in mice challenged for 3 weeks with a choline-deficient diet, (CDAA = choline-deficient L-amino acid defined) or a choline-supplemented control diet (CSAA = choline-supplemented L-amino acid defined). Lobular inflammation and hepatocyte ballooning scores for each mouse are listed in the table, and the average value of each parameter is indicated under the dash line. Scoring was performed in the same way as described in Table S1.

Table S3. Histopathologic analysis of effects of rFGF1 (6 weeks) on hepatic inflammation in choline-deficient mice.

	CSAA	CDAA	CDAA + rFGF1
Lobular inflammation	1(3) 1(2) 1(1) 0	2 (9) 2 (10) 1 (5) 2 (11) 1 (8)	2 (16) 3 (23) 2 (16) 3 (20)
	Average 0.75	**Average 1.6**	**Average 2.5**
Ballooning	0 1 1 0	1 1 1.5 1 1	1 1.5 1 1
	Average 0.5	**Average 1.1**	**Average 1.1**

Table S3. Histopathologic evaluation of the effect of rFGF1 on hepatic inflammation in mice challenged for 6 weeks with a choline-deficient diet, (CDAA = choline-deficient L-amino acid defined) or a choline-supplemented control diet (CSAA = choline-supplemented L-amino acid defined). Lobular inflammation and hepatocyte ballooning scores for each mouse are listed in the table, and the average value of each parameter is indicated under the dash line. Scoring was performed in the same way as described in Table S1.

Table S4. Histopathologic analysis of effects of rFGF1 (3 and 6 weeks) on proliferation in choline-deficient mice.

	CSAA		CDAA		CDAA + rFGF1	
3 week		1		12		2
		3		8		2
		1		6		13
		3		1		4
				11		3
	Average	2.0	Average	7.6	Average	4.8
6 week		26		15		1
		2		5		9
		15		5		5
		10		15		4
		2		3		
	Average	11.0	Average	8.6	Average	4.8

Table S4. Histopathologic evaluation of the effect of rFGF1 on hepatic proliferation in mice challenged for 3 or 6 weeks with a choline-deficient diet, (CDAA = choline-deficient L-amino acid defined) or a choline supplemented control diet (CSAA = choline supplemented L-amino acid defined). Proliferation is expressed as number of Ki-67 positive nuclei within 4 microscopic fields at 100x magnification per mouse liver.

References

1) Ahmed A, Wong RJ, Harrison SA (2015) NAFLD Review: Diagnosis, Treatment and Outcomes. *Clin Gastroenterol Hepatol* pii: S1542-3565.
2) Marchesini G, et al. (2003) Nonalcoholic fatty liver, steatohepatitis, and the metabolic syndrome. *Hepatology* 37:917-923.
3) Adams LA, Angulo P (2006) Treatment of non-alcoholic fatty liver disease. *Postgrad Med J* 82:315-322.
4) Tontonoz P, Spiegelman BM (2008) Fat and beyond: the diverse biology of PPARgamma. *Ann. Rev.* Biochem 77:289-312.
5) Kim HI, Ahn YH (2004) Role of peroxisome proliferator-activated receptor-gamma in the glucose-sensing apparatus of liver and beta-cells. *Diabetes* 53 Suppl 1:S60-5.
6) Jiang C, Ting AT, Seed B. (1998) PPAR-γ agonists inhibit production of monocyte inflammatory cytokines. *Nature* 391:82–86.
7) Ricote M, Li AC, Willson TM, Kelly CJ, Glass, CK (1998) The peroxisome proliferator-activated receptor-γ is a negative regulator of macrophage activation. *Nature* 391:79–82.
8) Jonker JW, et al. (2012) A PPARγ-FGF1 axis is required for adaptive adipose remodelling and metabolic homeostasis. *Nature* 485:391-394.
9) Suh JM, et al. (2014) Endocrinization of FGF1 produces a neomorphic and potent insulin sensitizer. *Nature* 513:436-439.
10) Park HS, et al. (2011) Time-dependent changes in lipid metabolism in mice with methionine choline deficiency-induced fatty liver disease. *Mol Cells* 32:571-577.
11) Wiegman CH, et al. (2003) Hepatic VLDL production in ob/ob mice is not stimulated by massive de novo lipogenesis but is less sensitive to the suppressive effects of insulin. *Diabetes* 52:1081-1089.
12) Anstee QM, Goldin RD (2006) Mouse models in non-alcoholic fatty liver disease and steatohepatitis research. *Int J Exp Pathol* 87:1-16.
13) Yu C, et al. (2003) Role of fibroblast growth factor type 1 and 2 in carbon tetrachloride-induced hepatic injury and fibrogenesis. *Am J Pathol* 163:1653-62.
14) Barrios R, et al. (1997) Upregulation of acidic fibroblast growth factor during development of experimental lung fibrosis. *Am J Physiol* 273:L451-8.
15) MacKenzie B, et al. (2015) Increased FGF1-FGFRc expression in idiopathic pulmonary fibrosis. *Respir Res* 2015 16:83.

16) Leask A, Abraham DJ (2004) TGF-beta signaling and the fibrotic response. *FASEB J* 18:816-827.
17) Miller ER, et al. (2005) Meta-analysis: high-dosage vitamin E supplementation may increase all-cause mortality. *Ann Intern Med* 142:37-46.
18) Bjelakovic G, Nikolova D, Gluud LL, Simonetti RG, Gluud C (2007) Mortality in randomized trials of antioxidant supplements for primary and secondary prevention: systematic review and meta-analysis. *JAMA* 297:842-857.
19) Nissen SE, Wolski K (2007) Effect of rosiglitazone on the risk of myocardial infarction and death from cardiovascular causes. *N Engl J Med* 356:2457-2471.
20) Balint BL, Nagy L (2006) Selective modulators of PPAR activity as new therapeutic tools in metabolic diseases. *Endocr Metab Immune Disord Drug Targets.* 6:33-43.
21) Potthoff MJ, Kliewer SA, Mangelsdorf DJ (2012) Endocrine fibroblast growth factors 15/19 and 21: from feast to famine. *Genes Dev* 26:312-324.
22) Holt JA, et al. (2003). Definition of a novel growth factor-dependent signal cascade for the suppression of bile acid biosynthesis. Genes Dev 17:1581-91.
23) Ito S, et al. (2005) Impaired negative feedback suppression of bile acid synthesis in mice lacking betaKlotho. *J Clin Invest* 115: 2202-2208.
24) Inagaki T., et al. (2005). Fibroblast growth factor 15 functions as an enterohepatic signal to regulate bile acid homeostasis. *Cell Metab* 2:217-25.
25) Potthoff MJ, et al. (2011) FGF15/19 regulates hepatic glucose metabolism by inhibiting the CREB-PGC-1α pathway. *Cell Metab* 13:729-738.
26) Jiang S et al. (2014) Fibroblast growth factor 21 is regulated by the IRE1α-XBP1 branch of the unfolded protein response and counteracts endoplasmic reticulum stress-induced hepatic steatosis. *J Biol Chem* 289:29751-29765.
27) Adams AC et al. (2012) The breadth of FGF21's metabolic actions are governed by FGFR1 in adipose tissue. *Mol Metab* 2:31-37.
28) Nakae D (1999) Endogenous liver carcinogenesis in the rat. *Pathol. Int* 49:1028-1042.
29) Hijmans BS, Grefhorst A, Oosterveer MH, Groen AK (2014) Zonation of glucose and fatty acid metabolism in the liver: mechanism and metabolic consequences. *Biochimie* 96:121-129.
30) Shoelson SE, Lee J, Goldfine AB (2006) Inflammation and insulin resistance. *J Clin Invest* 116:1793-801.
31) Trauner M, Arrese M, Wagner M. (2010) Fatty liver and lipotoxicity. *Biochim Biophys Acta* 1801:299-310.
32) Cusi K. (2012) Role of obesity and lipotoxicity in the development of nonalcoholic steatohepatitis: pathophysiology and clinical implications. *Gastroenterology* 142:711-725.
33) Lalor PF, Shields P, Grant A, Adams DH (2002) Recruitment of lymphocytes to the human liver. *Immunol Cell Biol* 80:52-64.
34) Zhang H, Issekutz AC (2002) Down-modulation of monocyte transendothelial migration and endothelial adhesion molecule expression by fibroblast growth factor. *Am J of Pathol* 160:2219-2230.
35) Steinhoff G, Behrend M, Schrader B, Duijvestijn AM, Wonigeit K (1993) Expression pattern of leukocyte adhesion ligand molecules on human liver endothelia: lack of ELAM-1 and CD62 inducibility on sinusoidal endothelia and distinct distribution of VCAM-1, ICAM-1, ICAM-2 and LFA-3. *Am J Pathol* 142:481-488.
36) Gebhardt R., Mecke D. (1983) Heterogeneous distribution of glutamine synthetase among rat liver parenchymal cells in situ and in primary culture. *EMBO J* 2:567-570.
37) Kleiner DE, et al. (2005) Nonalcoholic Steatohepatitis Clinical Research Network. Design and validation of a histological scoring system for nonalcoholic fatty liver disease. *Hepatology* 41:1313-1321.
38) Seglen PO (1976) Preparation of isolated rat liver cells. *Methods Cell Biol* 13:29-83.